Journal of Photochemistry and Photobiology A: Chemistry 217 (2011) 169–176

Contents lists available at ScienceDirect

Journal of Photochemistry and Photobiology A: Chemistry

journal homepage: www.elsevier.com/locate/jphotochem

Dye-sensitized solar cells employing amphiphilic poly(ethylene glycol) electrolytes

Rajkumar Patel [a], Jin Ah Seo [a], Joo Hwan Koh [a], Jong Hak Kim [a,*], Yong Soo Kang [b,**]

[a] Department of Chemical and Biomolecular Engineering, Yonsei University, 262 Seongsanno, Seodaemun-gu, Seoul 120-749, South Korea
[b] WCU Department of Energy Engineering, Hanyang University, Seoul 133-791, South Korea

ARTICLE INFO

Article history:
Received 21 January 2010
Received in revised form
17 September 2010
Accepted 5 October 2010
Available online 14 October 2010

Keywords:
Polymer electrolyte
Dye-sensitized solar cell
Amphiphilic polymer
Spectroscopy
Poly(ethylene glycol)

ABSTRACT

Poly(ethylene glycol) (PEG) was modified with a long alkyl acid to produce a self-organized amphiphilic polymer (amPEG). FT-IR and NMR spectroscopies confirmed the amPEG synthesis. This polymer was complexed with lithium iodide (LiI) and 1-methyl-3-propylimidazolium iodide (MPII) to prepare polymer electrolytes to be applied to dye-sensitized solar cells (DSSC). FT-IR studies showed that upon the addition of litium salt the free ether and ester carbonyl bands shifted towards lower wavenumbers, indicating the complexation of Li ions with oxygens on the amPEG. Alkylation and salt introduction reduced PEG crystallinity, as characterized by wide angle X-ray scattering (WAXS) and differential scanning calorimetry (DSC). The ionic conductivities of the polymer electrolytes increased with increasing salt concentrations, and the energy conversion efficiency of DSSC reached 2.6% at 100 mW cm^{-2} for amPEG/MPII system which is higher than amPEG/LiI. This may be due to the higher mobility of MPII ion than the lithium ion in the polymer electrolyte. The interfacial properties between electrolytes and electrodes were investigated using field-emission scanning electron microscopy (FE-SEM) and electrochemical impedance spectroscopy (EIS).

1. Introduction

Dye-sensitized solar cells (DSSCs) have higher energy conversion efficiencies (~11% at 1 sun AM 1.5) and 80% lower production costs than do silicone solar cells [1–7]. Liquid electrolytes containing redox couples are commonly used for DSSC [8,9]. These solar cells require the formation of a perfect seal to avoid solvent evaporation, leakage, high temperature instabilities and flammabilitiy. There have been many attempts to substitute liquid electrolytes into DSSCs with solid or quasi-solid state electrolytes [10–24]. Among these attempts, DSSCs employing polymer electrolytes have received great interest [10,11,25–28].

Poly(ethylene glycol) (PEG) is one polymer that has attracted much attention in polymer electrolytes because of its high polarity, its ability to dissolve redox couples and its excellent chemical stability. The ionic conductivities of PEG-based electrolytes are somewhat limited due to their high crystallinities. As a result, much research has attempted to increase ionic conductivity by modifying PEG [10–12]. For example, Kang et al. modified PEG via cross-linking based on polyurethane synthesis, and Chatzivasiloglou et al. used propylene carbonate as a PEG plasticizer [29–31].

A high ionic conductivity of polymer electrolytes is considered essential, but ionic conductivity usually decreases with increasing mechanical strength because both parameters are strongly related to polymer chain movement. Self-organized, microphase-separated polymers can offer both high ionic conductivity and dimensional stability and thus have recently attracted interest for use in polymer electrolytes [32,33].

Studies have demonstrated the importance of interfacial contact between polymer electrolytes and dye-adsorbed semiconductors [26–28]. Electrolyte penetration through the photoelectrode nanopores is essential for obtaining good photovoltaic performances of DSSCs composed of polymer electrolytes. As a result, the sizes of polymer chains and pore diameters should be adequately matched for deeper penetration of polymer electrolytes into TiO_2 nanopores. The coil sizes of polymer chains are commonly represented by the radius of gyration, R_g, expressed approximately by $R_g = C(M_w)^{0.5}$, where M_w is the molecular weight in g/mol and $C = 0.063$ nm/(g/mol)$^{0.5}$ for poly(ethylene oxide) (PEO) in a good solvent [34]. Thus, in the case of PEG or its derivatives, using a lower molecular weight compound is referred to as the "oligomer approach". Another approach is "fabrication of an ionic path", which employs carbon nanotubes and nanoparticles, as reported by Usui et al. [35]. Kato et al. also used dicarboxylic acids having 6, 10 or 12 carbon atoms chemically linked to TiO_2 nanoparticles by esterification at higher temperature [36]. They also reported TiO_2 esterified with long chain bromoacid and in turn linked to immidazolium ions

* Corresponding author. Tel.: +82 2 2123 5757; fax: +82 2 312 6401.
** Co-corresponding author.
E-mail addresses: jonghak@yonsei.ac.kr (J.H. Kim), kangys@hanyang.ac.kr (Y.S. Kang).

1010-6030/$ – see front matter © 2010 Elsevier B.V. All rights reserved.
doi:10.1016/j.jphotochem.2010.10.005

for the enhancement of short circuit current (J_{sc}) by fabricating an ionic path between nanoparticles [37].

In this work, PEG was modified with a long alkyl acid to produce a self-organized amphiphilic polymer that can provide high ionic conductivity with good mechanical properties. Alkylation is expected to help reduce PEG crystallinity and to enhance the mechanical strength of the polymer electrolyte. Polymer electrolytes consisting of amphiphilic PEG, metal salt (LiI) or ionic liquid (1-methyl-3-propylimidazolium iodide, MPII), and I_2 were prepared and applied to DSSCs. The resultant materials were characterized using FT-IR, NMR spectroscopy, wide angle X-ray scattering (WAXS), differential scanning calorimetry (DSC) and field-emission scanning electron microscopy (FE-SEM).

2. Experimental

2.1. Materials

Poly(ethylene glycol) with two different molecular weights (1000 and 2000 g/mol), 6-bromohexanoic acid (BHA), 1-methyl-3-propylimidazolium iodide (MPII), lithium iodide (LiI), and amberlyst 15 (a cation exchange resin) were purchased from Aldrich chemicals and were used as received, without further purification.

2.2. Amphiphilic PEG synthesis

Three grams of PEG 1000 g/mol (1k) or 2000 g/mol (2k) was dissolved in 15 mL of tetrahydrofurane (THF) in a 250 mL round bottom flask via stirring. In a separate vessel, 3 g 6-bromohexanoic acid (BHA) was dissolved in 15 mL THF and added to the PEG solution. To the reaction mixture, 0.75 g amberlyst 15 was added. The reaction mixture was refluxed at 85 °C for 5 h. The product was isolated using hexane and dried in a vacuum oven.

2.3. Polymer electrolyte preparation

Synthesized amphiphilic PEGs with two different molecular weights (1000 and 2000 g/mol) were used as polymer matrices. Lithium iodide salt or MPII ionic liquid was used as an iodide source. The molar ratios of the oxygen atoms to salt cations in the polymers were 20:1, 10:1 and 5:1. The iodine content was fixed at 10 mol% with respect to LiI or MPII.

2.4. Preparation of photoelectrodes

Transparent glass, coated with conductive FTO, was used for the photoelectrode. The neat glass was cleaned by sonication in isopropanol and then in chloroform. The clean conducting surface of the FTO glass was blocked by a layer of titanium(IV) bis (ethyl acetoacetato) diisopropoxide using spin coating, followed by heating to 450 °C for 2 h, holding for 30 min, and cooling to 30 °C for 4 h. Then, commercialized TiO_2 paste (Ti-Nanoxide T, Solaronix) was cast onto the FTO glass by a doctor-blade technique and successive sintering at 450 °C for 30 min. The nanocrystalline TiO_2 film (with a thickness of ca. 12 μm) was sensitized overnight with a $Ru(dcbpy)_2(NCS)_2$ dye (dcbpy = 2,2-bipyridyl-4,4-dicarboxylato) solution (535-bisTBA, Solaronix, 13 mg dissolved in distilled ethanol (50 g)).

2.5. Preparation of counter electrode

Transparent glasses coated with a conductive FTO were used for counter electrodes. These glasses were cleaned by sonication in isopropanol and then in chloroform. The counter electrodes were prepared by spin coating 4 wt% H_2PtCl_6 2-propanol solution onto the conductive FTO glass and sintering at 450 °C for 2 h, holding for 30 min, and cooling to 30 °C over 8 h.

2.6. Fabrication of DSSC

DSSCs with an active area of 0.4 cm^2 were constructed by drop-casting of electrolyte solution onto the photoelectrode and covering with the counter electrode, according to previous reported procedure [26–30]. The cells were placed in a vacuum oven for a day to permit complete evaporation of solvent and were then sealed with an epoxy resin. Photoelectrochemical performance characteristics, including short-circuit current (J_{sc}, mA cm^{-2}), open-circuit voltage (V_{oc}, V), fill factor (ff), and overall energy conversion efficiency (η) were measured using a Keithley Model 2400 and a 1000 W xenon lamp (Oriel, 91193). The light was homogeneous over an 8 in. × 8 in. area, and its intensity was calibrated with a Si solar cell (Fraunhofer Institute for Solar Energy System, Mono-Si + KG filter, Certificate No. C-ISE269) for a sun light intensity of 1 (100 mW cm^{-2}). This calibration was double-checked with a NREL-calibrated Si solar cell (PV Measurements Inc.).

2.7. Characterization

Proton nuclear magnetic resonance (^{1}H NMR) measurements were performed with a 600-MHz, high-resolution NMR spectrometer (Avance 600-MHz FT-NMR spectrometer, Bruker, Ettlingen, Germany). Fourier transfer infrared (FTIR) spectra of samples were collected with an Excalibur series FTIR (DIGLAB, Co., Hannover, Germany) in the 4000–600 cm^{-1} frequency range with an attenuated total reflection facility. The polymer thermal properties were investigated using a differential scanning calorimeter (DSC Q2000 from TA Instruments). The sample was heated in nitrogen at 10 °C/min from −85 °C to 120 °C. The sample was then cooled to −85 °C and heated to 120 °C again, following the same procedure. The second scan thermogram determined the transition temperatures of the polymer and polymer electrolytes. Morphological characterization for the nanocrystalline TiO_2 layer was carried out using a field-emission scanning electron microscope (FE-SEM, S-4700, Hitachi). Ionic conductivity was measured using a two-point probe conductivity cell.

3. Results and discussion

3.1. Amphiphilic PEG (amPEG) synthesis

The synthesis procedure for amPEG is presented in Scheme 1. In this process, hydrophilic PEG was esterified with BHA to produce a self-organized amphiphilic polymer containing long hydrophobic alkyl groups at the ends, as characterized by FT-IR and NMR spectroscopies. Fig. 1 shows FT-IR spectra of pristine and 2000 g/mol PEG (PEG_{2k}), HPA and amPEG. The free hydroxyl band of PEG at 3388 cm^{-1} shifted to 3446 cm^{-1}, and the carbonyl peak of BHA at 1685 cm^{-1} shifted to 1730 cm^{-1}, implying successful esterification. Fig. 2 shows the ^{1}H NMR spectrum of amphiphilic PEG (2000 g/mol) esterified with BHA. Peaks below 2 ppm indicate the methylene proton of BHA. Peaks a and b represent methylene protons adjacent to the ester group and bromine, respectively. The ethylene oxide protons appear at 3.65 ppm, which is assigned as peak c. The ethylene oxide peak shifted downfield to 4.22 ppm and was assigned as peak d. These spectroscopic results indicate the successful esterification of PEG [38] to produce amPEG with hydrophilic and hydrophobic segments.

3.2. Coordinative interactions of the polymer electrolytes

The coordinative interactions of immidazolium ions with the ester and ether oxygens on amPEG were investigated using FT-IR

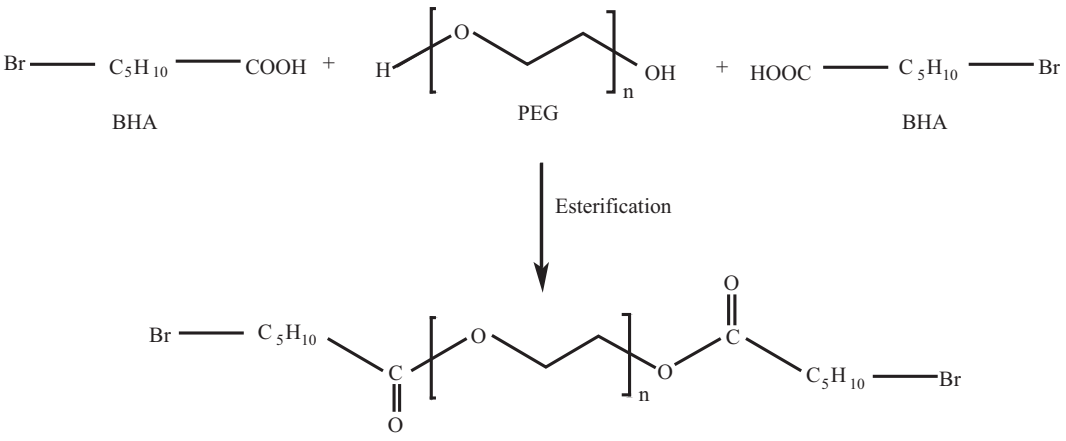

Scheme 1. Synthesis of amphiphilic PEG (amPEG) containing alkyl groups.

spectroscopy, as presented in Fig. 3. The carbonyl (C=O) stretching band of amPEG appeared at 1730 cm^{-1}. For the polymer electrolyte with a 5:1 molar ratio, this peak appeared at around same wavenumber, but with a lower intensity, indicating some interaction with the immidazolium ion. In addition, the C–O–C stretching band of the ester group in amPEG at 1107 cm^{-1} remains almost unchanged, implying no significant interaction between immidazolium ions and the C–O–C oxygen.

Fig. 4 shows FT-IR spectra of neat LiI, amPEG and amPEG/LiI/I_2 with different salt contents. The carbonyl band of the ester group appeared at 1727 cm^{-1} with a very low intensity in the 5:1 polymer electrolyte compared to that in the pristine amPEG. In addition,

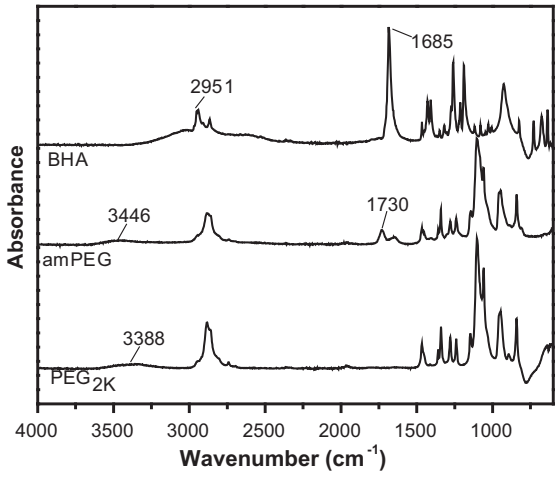

Fig. 1. FT-IR spectra of PEG_{2k}, BHA and amPEG.

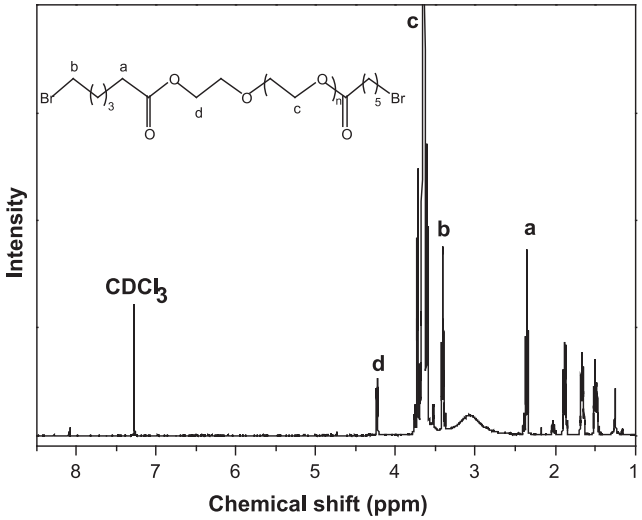

Fig. 2. ^1H NMR spectrum of amPEG.

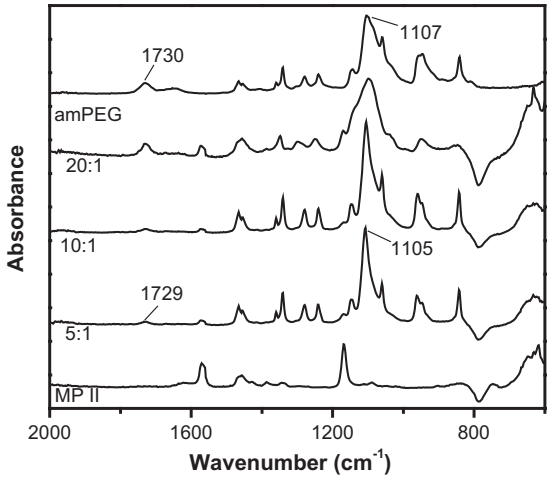

Fig. 3. FT-IR spectra of amPEG, MPII and amPEG/MPII/I_2 from 20 to 5% MPII compositions.

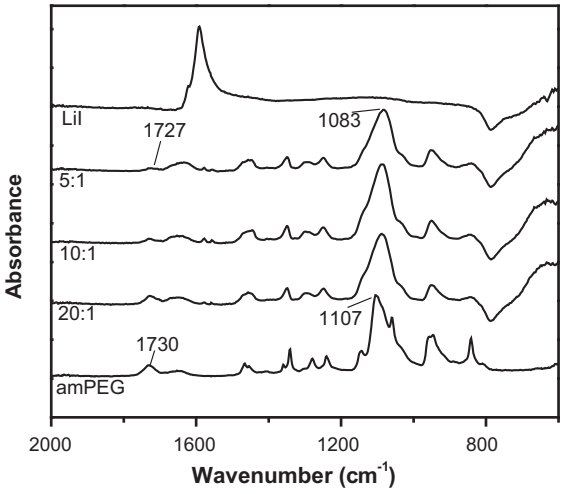

Fig. 4. FT-IR spectra of LiI, amPEG and amPEG/LiI/I_2 from 20 to 5% LiI compositions.

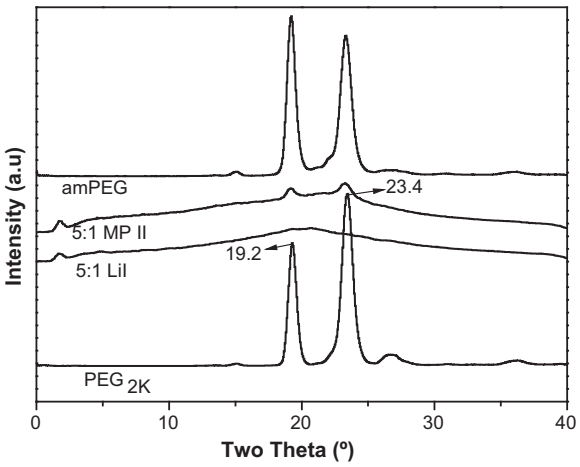

Fig. 5. WAXS results of PEG_{2k}, amPEG, amPEG/LiI/I_2 and amPEG/MPII/I_2.

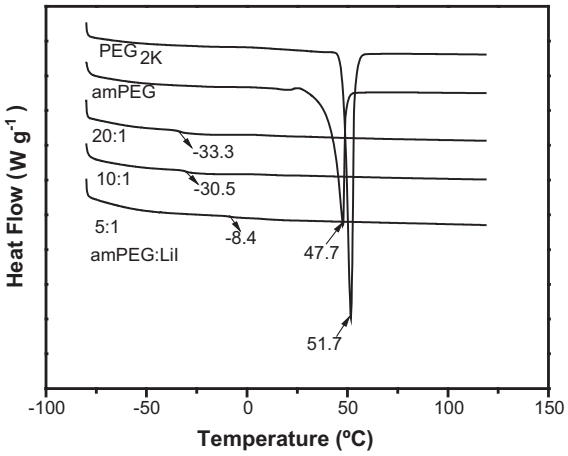

Fig. 6. DSC thermograms of PEG_{2k}, amPEG and amPEG/LiI/I_2 with different compositions.

the C–O–C stretching band shifted significantly from 1107 to 1083 cm^{-1}. These results demonstrate that lithium ions interact with the C=O or C–O–C oxygens, but mostly coordinate with the ether (C–O–C) oxygens. The shift to a lower wavenumber originates from loosening of the C–O or C=O bonds via electron donation to salt cations [26,29].

3.3. Structural changes in the polymer electrolytes

Ionic diffusion in polymer electrolytes is well known to depend on structural properties such as chain rigidity and free volume. The WAXS patterns for PEG_{2k}, amPEG, amPEG/LiI/I_2 and amPEG/MPII/I_2 with a 5:1 molar composition were obtained to investigate the structural changes in PEG and the dissolution behaviors of inorganic materials such as LiI, MPII and I_2 (Fig. 5). The PEG and amPEG polymer samples exhibited two strong crystalline peaks at 19.2° and 23.4°, but their relative intensities differed. The two peaks are due to the typical 7/2 helical structure of polyethylene glycol, that is, seven ethylene oxide repeat units with two turns in a fiber period of 1.93 nm [39,40]. Upon adding LiI to amPEG at a 5:1 ratio, two sharp crystalline PEG peaks disappeared and LiI was absent, indicating complete LiI salt dissolution in the polymer matrix. Two small PEG crystalline peaks remained in the polymer electrolyte containing MPII ionic liquid, demonstrating some intact crystallinity and reduced interaction between the polymer and ionic liquid compared to that of the LiI salt. The degrees of crystallinity calculated from WAXS plots and DSC are presented in Table 1. The amPEG crystallinity was 71.4%, which decreased to 2.3% in the amPEG/MPII/I_2 5:1 system. Thus, polymer matrices have weaker interactions with MPII than with lithium metal salt.

The DSC thermograms for PEG_{2k}, amPEG and amPEG/LiI/I_2 with different compositions are presented in Fig. 6. The glass transition temperature (T_g) of pristine PEG (PEG_{2k}) was not accurately observed in our work but is near −70 °C according to the literature [41]. The crystalline melting point (T_m) of pristine PEG was 51.7 °C and that of amPEG was 47.7 °C. Upon increasing salt concentration from 20:1 to 5:1 in amPEG/LiI/I_2, the T_g value continuously increased from −33.3 °C to −8.4 °C. This result strongly indicates a coordinative interaction between the LiI salt and the polymer matrix, resulting in a restricted chain mobility. Another indication of the strong interaction between the salt and the polymer matrix is the absence of T_m in all compositions.

The DSC measurements for the amPEG/MPII/I_2 system with varying compositions and the resulting thermograms are presented in Fig. 7. The T_g of the amPEG/MPII/I_2 electrolyte at 20:1 was −60.4 °C. T_g increased continuously and reached −58.6 °C for the 5:1 composition. Considering the 1.8 °C rise in T_g, which is very marginal, the interactions between the MPII ionic liquid and the polymer matrix are much weaker than those between the LiI salt and the polymer matrix, consistent with the FT-IR and WAXS results. The crystalline melting temperature in amPEG was 47.7 °C. For the 20:1 composition, T_m decreased to 27.7 °C; however, increasing the MPII concentration to 5:1 intriguingly increased T_m to 39.1 °C, implying less favorable interactions at higher salt concentrations. Unlike the interaction between amPEG and LiI salt in the amPEG/LiI/I_2 electrolyte, the amPEG crystallinity in the amPEG/MPII/I_2 remains intact, which demonstrates a reduced interaction between amPEG and MPII. The degrees of crystallinity (X_c) were quantitatively determined using the DSC thermogram [42] and are presented in Table 1. The degree of PEG crystallinity,

Table 1
Degrees of crystallinity as determined by WAXD and DSC.

Sample	Crystallinity % (WAXD study)	Crystallinity % (DSC study)
PEG_{2k}	80.5	84.3
amPEG	71.4	75.8
amPEG/MPII/I_2 (20:1)	–	11.8
amPEG/MPII/I_2 (10:1)	–	38.3
amPEG/MPII/I_2 (5:1)	2.3	10.6
amPEG/LiI/I_2	–	–

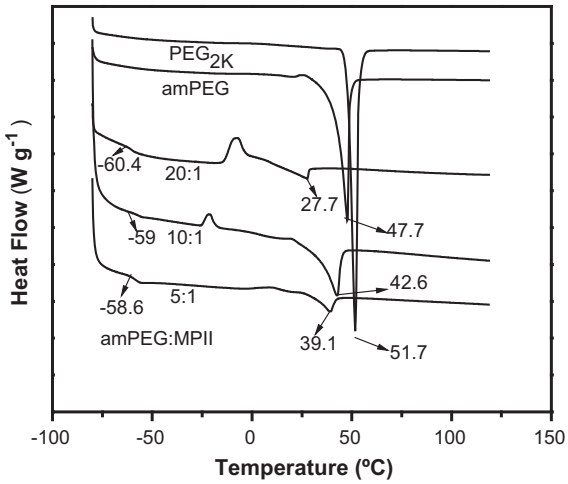

Fig. 7. DSC thermograms of PEG_{2k}, amPEG and amPEG/MPII/I_2 with different compositions.

as calculated from the DSC plot, was about 84.3%. After PEG esterification by BHA, the crystallinity decreased to 75.8% (amPEG). The polymer electrolyte crystallinity decreased from 11.8% for the 20:1 composition to 10.6% for the 5:1 composition, indicating limited interaction between amPEG and the immidazolium ion. In the amPEG/LiI/I_2 system, the DSC thermogram showed no melting transition peak irrespective of composition, suggesting a loss of PEG crystallinity and an intimate interaction between the lithium ion and the polymer matrix amPEG. These results were consistent with those of the WAXS and FT-IR data.

3.4. Conducting and electrochemical properties

The impedance spectra of the amPEG/LiI/I_2 and amPEG/MPII/I_2 electrolytes were measured using the two-electrode method to investigate the ionic conductivities of the polymer electrolytes. The ionic conductivity in this study was calculated from the bulk resistance value found in the complex impedance diagram. The ionic conductivities of amPEG/MPII/I_2 electrolytes increased with increasing ionic liquid concentration in the range of 10^{-6}–10^{-5} S cm^{-1}. In the case of amPEG/LiI/I_2 electrolytes, the increased ionic conductivities with increased metal ion concentration are less prominent in the region of 10^{-7} S cm^{-1} than are those produced in the interactions with ionic liquid. As the FT-IR, WAXS and DSC studies showed that there is better coordinative interaction between the lithium ion with the oxygen atom of amPEG in amPEG/LiI electrolyte than the ionic liquid ion in amPEG/MPII electrolyte. As a result, the stiffness of the polymeric chain increases and decreases the electronic diffusion of I_3^- in the amPEG/LiI electrolyte. This results in the decrease of the ionic conductivity of lithium ion in amPEG/LiI electrolyte as compared to amPEG/MPII electrolyte. At the same time, the SEM image showed better interfacial for MP II electrolyte system than LiI electrolyte resulting in higher conductivity for amPEG/MPII [43,44].

Polymer electrolyte penetration into dye-attached nanoporous TiO_2 nanoparticles triggers intimate contact which governs the ionic mobility and most importantly the overall conversion efficiency of DSSC [23,24]. Kang et al. studied the PEG-based polymer electrolyte in detail, suggesting that the coil size of the electrolyte medium should be smaller than the average pore of diameter of the TiO_2 layers [30]. Therefore, PEG should be used with a M_w = 2000 (R_g = 2.82 nm) or lower, which was the basis for the decision to use PEG_{2k} and PEG_{1k} (R_g = 1.99 nm) in this study. Furthermore, these polymers were esterified with long chain bromo acid to create ionic paths [36,37]. Fig. 8 shows cross-sectional FE-SEM photomicrographs of the pristine TiO_2 electrode and the TiO_2 electrode with amPEG/LiI/I_2 and amPEG/MPII/I_2 (5:1). The dye-attached TiO_2 nanoparticles have particle diameters around 20–30 nm. When lithium iodide salt containing amPEG electrolyte was introduced, the nanocrystalline TiO_2 particles seemed to be

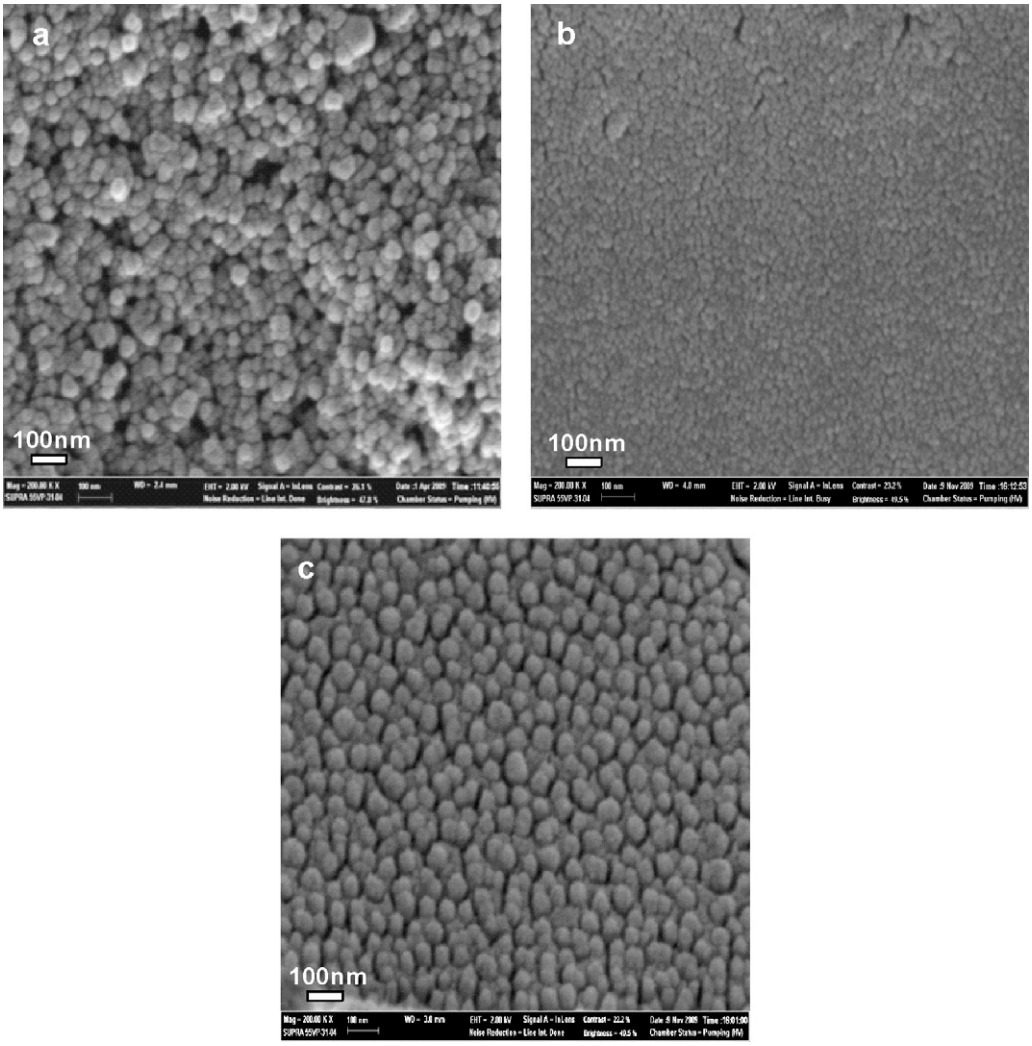

Fig. 8. Cross-sectional FE-SEM images indicating the penetration of polymer electrolytes in a (a) pristine TiO_2 electrode, (b) TiO_2 electrode with amPEG/LiI/I_2 (5:1), and (c) TiO_2 electrode with amPEG/MPII/I_2 (5:1).

Table 2
Photovoltaic performances of open-circuit voltage (V_{oc}), short-circuit current (J_{sc}), fill factor (ff) and overall energy conversion efficiency (η).

Polymer electrolyte (5:1)	V_{oc} (V)	J_{sc} (mA cm^{-2})	ff	Efficiency (%)	R1 (Ω)	R2 (Ω)	Dark R (Ω)
amPEG$_{1k}$/MPII/I$_2$	0.56	8.0	0.53	2.3	84	170	2130
amPEG$_{1k}$/LiI/I$_2$	0.40	9.9	0.47	1.9	100	130	28,000
amPEG$_{2k}$/MPII/I$_2$	0.57	8.1	0.58	2.6	80	120	1605
amPEG$_{2k}$/LiI/I$_2$	0.42	7.7	0.57	1.8	92	300	10,000

adequately coated with polymer electrolyte, resulting in good penetration of the electrolyte material into the nanopores, as shown in Fig. 8(b). Adding amPEG with MPII electrolyte improved the interfacial contact between the TiO_2 nanoparticles and the electrolyte, as shown in Fig. 8(c). The TiO_2 nanoparticle size increased to around 65–70 nm as a result of polymer electrolyte adsorption onto the surface.

The photovoltaic performances of DSSCs fabricated with amPEG (M_w = 1 and 2 kg/mol), MPII ionic liquid or LiI salt and I_2 as the redox system were evaluated using J–V measurements, as shown in Fig. S1 (Supporting information). The cell performances including η, ff, V_{oc} and J_{sc} of DSSCs employing amPEG, LiI and MPII electrolytes are summarized in Table 2. The amPEG electrolytes containing MPII exhibited higher efficiency than did those containing LiI salt, which is expected, due to the higher mobility of the electrolyte. Strong coordination interaction of lithium ion with the polar oxygen atom in amPEG/LiI electrolyte than MPII ion in amPEG/MPII electrolyte resulted in higher transient crosslinking of polymer chain and thus higher increase of T_g in the former (by 25 °C) than in the latter (by 2 °C). This will lead to the decrease in diffusion coefficient of I_3^- in amPEG/LiI electrolytes [43,44]. As a result, the efficiency of amPEG/LiI/I_2 electrolyte was approximately 75% lower than that of the amPEG/MPII/I_2.

The internal resistances and electron transport kinetics of the TiO_2 films in DSSC were studied using EIS analysis. Fig. 9 shows the Nyquist plots of EIS for DSSCs with different compositions measured at 100 mW cm^{-2}. Usually, all DSSC spectra exhibit three semicircles, which are assigned to electrochemical reactions at the Pt counter electrode, the charge transfer at the TiO_2/dye/electrolyte and the Warburg diffusion process of I^-/I_3^- [45,46]. The first semicircle in the high frequency range is primarily related to the sheet resistance of FTO and remains nearly constant regardless of the system. In our case the sheet resistance is too small to be recognized and almost merge in the second semicircle. The second semicircle is attributed to the impedance in the counter electrode/redox electrolyte interface (R1). The largest semicircle in the low frequency range represents the impedance associated with the charge transfer between the dye-sensitized TiO_2 and the electrolyte interface (R2). The charge transport resistance at the TiO_2/dye/electrolyte interface decreased from amPEG$_{1k}$/LiI/I_2 to amPEG$_{2k}$/MPII/I_2, as seen in Fig. 10 and Table 2. This phenomenon may be due to the lower ionic mobility of the polymer electrolyte containing LiI compared to that containing MPII ionic liquid. Similarly, the characteristic frequency peaks (10^{-2}–10^6 Hz) in the Bode phase plots are shown in Fig. 10. The characteristic peak shifted to a lower frequency when the polymer electrolyte salt changed from lithium salt to MPII ionic liquid. The characteristic frequency is related to the inverse of the recombination lifetime (τ_r), or electron lifetime (τ_e), in the TiO_2 film [47,48]. This indicates that an ionic liquid containing polymer electrolyte has a longer electron lifetime in the TiO_2 photoelectrode. These results imply that electrolytes containing lithium salt have higher resistances and lower electron lifetimes in photoelectrodes.

Electrochemical impedance spectroscopy was also conducted in the dark to elucidate the correlation between electron transport and composition. In these cells, electrons were transported through the interconnected TiO_2 network and reacted with I_3^-. Simultaneously, I^- was oxidized to I_3^- at the counter electrode. Hence, the net current depended largely on the applied bias. Nyquist plots of the EIS in the DSSCs for different compositions measured in the dark are shown in Fig. 11 and Table 2. The DSSCs show very high resistance and only one peak. The resistance decreases from the lithium salt containing polymer electrolyte to the ionic liquid electrolytes, which may be due to the lower ionic mobility of the electrolytes of the lithium ion electrolyte. The Bode phase plots of characteristic frequency peaks (10^{-2}–10^6 Hz) measured in the dark are shown in Fig. S2 (Supporting information). The characteristic frequency peak appears only in one peak, unlike that observed in light conditions. The peak shifted to a lower frequency when the polymer electrolyte content changed from LiI salt to MPII ionic liquid, indi-

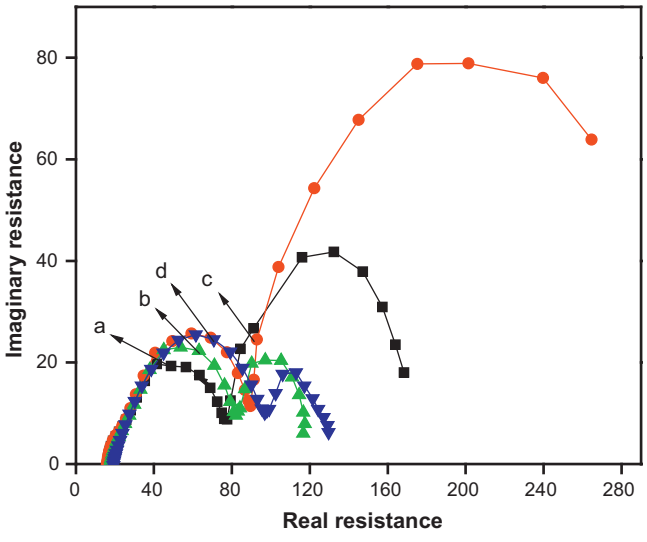

Fig. 9. Nyquist plots of DSSCs based on different compositions (a) amPEG$_{2k}$/MPII/I_2, (b) amPEG$_{1k}$/MPII/I_2, (c) amPEG$_{2k}$/LiI/I_2 and (d) amPEG$_{1k}$/LiI/I_2 at 100 mW cm^{-2}.

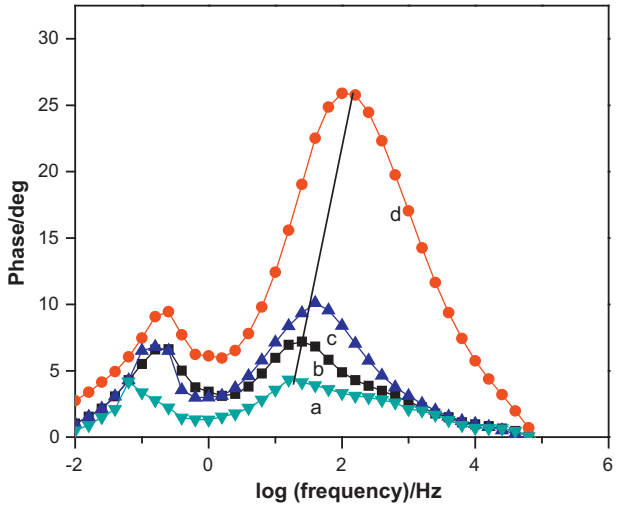

Fig. 10. Bode phase plots of DSSCs based on different compositions of (a) amPEG$_{2k}$/MPII/I_2, (b) amPEG$_{1k}$/MPII/I_2, (c) amPEG$_{2k}$/LiI/I_2 and (d) amPEG$_{1k}$/LiI/I_2 at 100 mW cm^{-2}.

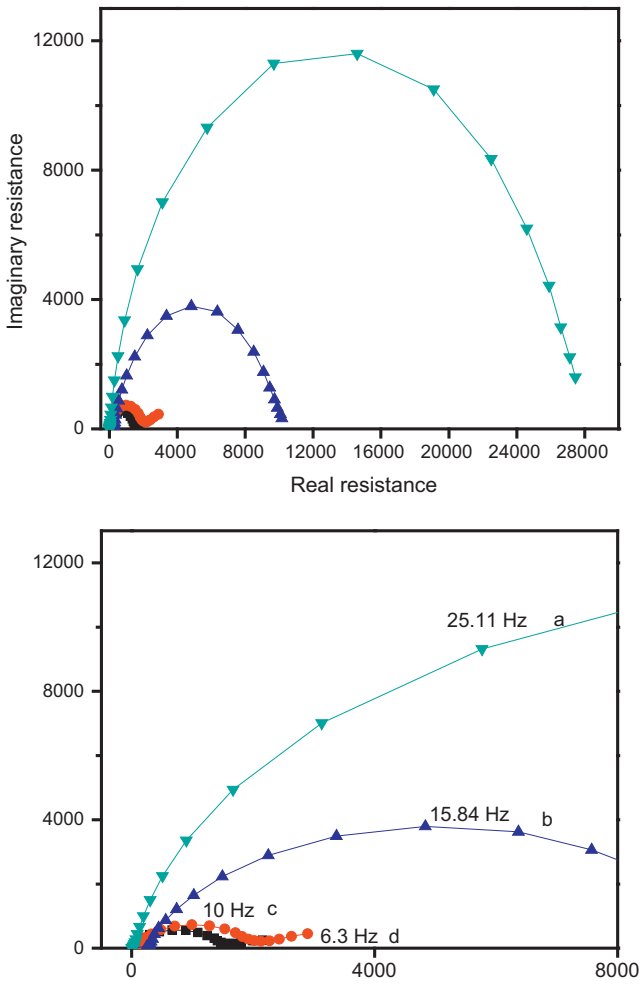

Fig. 11. EIS of DSSCs based on different compositions of (a) amPEG$_{2k}$/MPII/I_2 (15.84 Hz), (b) amPEG$_{1k}$/MPII/I_2 (24.54 Hz), (c) amPEG$_{2k}$/LiI/I_2 (38.9 Hz) and (d) amPEG$_{1k}$/LiI/I_2 (100 Hz) in the dark. (A) Nyquist plots and (B) enlarged Nyquist plots.

cating an increased lifetime for MPII-containing electrolytes and a higher resistance in the lithium salt electrolyte.

4. Conclusions

AmPEG was synthesized by modification of PEG which was used as a polymer matrix to prepare polymer electrolytes for TiO_2-based DSSC. The interaction between the ether and ester oxygen atoms in the polymer and the lithium ion from LiI salt or the immidazolium ion from MPII was characterized by FT-IR, WAXS and DSC. FT-IR results showed lower ester and ether peaks for the pristine amPEG, indicating coordinative interactions among the polymer electrolytes. According to WAXS and DSC analyses, increased salt content in amPEG reduced the polymer crystallinity to a considerable extent, unlike in ionic liquid systems. The conversion efficiency of amPEG/MPII/I_2 was 2.6% at 100 mW cm^{-2}. By increasing the MPII or LiI concentration the ionic conductivities of polymer electrolytes increased but compared to the amPEG/LiI system amPEG/MPII has higher ionic conductivity due to the higher mobility of MPII ion. The EIS technique was used to measure charge transport resistance and electron lifetime. The charge transport resistance in the TiO_2/dye/electrolyte decreased from salt to ionic liquid containing electrolytes as well as shift in the characteristic frequency towards lower value, indicating a higher electron lifetime. FE-SEM showed good interfacial contact between the polymer electrolytes and the nanoporous TiO_2 electrode.

Acknowledgements

This work was supported by the National Research Foundation (NRF) grant funded by the Korea Government (MEST) through the Korea Center for Artificial Photosynthesis (KCAP) located at Sogang University (NRF-2009-C1AAA001-2009-0093879) and the Center for Next Generation Dye-sensitized Solar Cells (No. 2010-0001842).

Appendix A. Supplementary data

Supplementary data associated with this article can be found, in the online version, at doi:10.1016/j.jphotochem.2010.10.005.

References

[1] B. O'Regan, M. Gratzel, A low-cost, high-efficiency solar cell based on dye-sensitized colloidal TiO_2 films, Nature 353 (1991) 737–740.
[2] U Bach, D. Lupo, P. Comte, J.E. Moser, F. Weissortel, J. Salbeck, H. Spreitzer, M. Gratzel, Solid-state dye-sensitized mesoporous TiO_2 solar cells with high photon-to-electron conversion efficiencies, Nature 395 (1998) 583–585.
[3] Y. Chen, E. Stathatos, D.D. Dionysiou, Sol–gel modified TiO_2 powder films for high performance dye-sensitized solar cells, J. Photochem. Photobiol. A: Chem. 203 (2009) 192–198.
[4] K. Hara, T. Sato, R. Katoh, A. Furube, Y. Ohga, A. Shinpo, S. Suga, K. Sayama, H. Sugihara, H. Arakawa, Molecular design of coumarin dyes for efficient dye-sensitized solar cells, J. Phys. Chem. B 107 (2003) 597–606.
[5] J. Kallioinen, M.R. Hassan, G.S. Paraoanu, J. Korppi-Tommola, Dye-sensitized nanostructured TiO_2 film based photoconductor, J. Photochem. Photobiol. A: Chem. 195 (2008) 352–356.
[6] H. Santa-Nokki, S. Busi, J. Kallioinen, M. Lahtinen, J. Korppi-Tommola, Quaternary ammonium polyiodides as ionic liquid/soft solid electrolytes in dye-sensitized solar cells, J. Photochem. Photobiol. A: Chem. 186 (2007) 29–33.
[7] M. Gratzel, Conversion of sunlight to electric power by nanocrystalline dye-sensitized solar cells, J. Photochem. Photobiol. A: Chem. 164 (2004) 3–14.
[8] B.A. Gregg, S.-G. Chen, S. Ferrere, Enhanced dye-sensitized photoconversion efficiency via reversible production of UV-induced surface states in nanoporous TiO_2, J. Phys. Chem. B 107 (2003) 3019–3029.
[9] S. Kambe, S. Nakade, T. Kitamura, Y. Wada, S. Yanagida, Influence of the electrolytes on electron transport in mesoporous TiO_2-electrolyte systems, J Phys. Chem. B 106 (2002) 2967–2972.
[10] T. Stergiopoulos, I.M. Arabatzis, G. Katsaros, P. Falaras, Binary polyethylene oxide/titania solid-state redox electrolyte for highly efficient nanocrystalline TiO_2 photoelectrochemical cells, Nano Lett. 2 (2002) 1259–1261.
[11] A.F. Nogueira, J.R. Durrant, M.-A. De Paoli, Dye-sensitized nanocrystalline solar cells employing a polymer electrolyte, Adv. Mater. 13 (2001) 826–830.
[12] G. Katsaros, T. Stergiopoulos, I.M. Arabatzis, K.G. Papadokostaki, P. Falaras, A solvent-free composite polymer/inorganic oxide electrolyte for high efficiency solid-state dye-sensitized solar cells, J. Photochem. Photobiol. A: Chem. 149 (2002) 191–198.
[13] W. Kubo, K. Murakoshi, T. Kitamura, S. Yoshida, M. Haruki, K. Hanabusa, H. Shirai, Y. Wada, S. Yanagida, Quasi-solid-state dye-sensitized TiO_2 solar cells: effective charge transport in mesoporous space filled with gel electrolytes containing iodide and iodine, J. Phys. Chem. B 105 (2001) 12809–12815.
[14] W. Kubo, S. Kambe, S. Nakade, T. Kitamura, K. Hanabusa, Y. Wada, S. Yanagida, Photocurrent-determining processes in quasi-solid-state dye-sensitized solar cells using ionic gel electrolytes, J. Phys. Chem. B 107 (2003) 4374–4381.
[15] E. Stathatos, P. Lianos, U. Lavrencic-Stangar, B. Orel, A high-performance solid-state dye-sensitized photoelectrochemical cell employing a nanocomposite gel electrolyte made by the sol–gel route, Adv. Mater. 14 (2002) 354–357.
[16] D. Gebeyehu, C.J. Brabec, N.S. Sariciftci, D. Vangeneugden, R. Kiebooms, D. Vanderzande, F. Kienberger, H. Schindler, Hybrid solar cells based on dye-sensitized nanoporous TiO_2 electrodes and conjugated polymers as hole transport materials, Synth. Met. 125 (2002) 279–287.
[17] O.A. Ileperuma, M.A.K.L. Dissanayake, S. Somasundaram, Dye-sensitised photoelectrochemical solar cells with polyacrylonitrile based solid polymer electrolytes, Electrochim. Acta 47 (2002) 2801–2807.
[18] P. Wang, S.M. Zakeeruddin, J.E. Moser, M.K. Nazeeruddin, T. Sekiguchi, M. Gratzel, A stable quasi-solid-state dye-sensitized solar cell with an amphiphilic ruthenium sensitizer and polymer gel electrolyte, Nat. Mater. 2 (2003) 402–407.
[19] D. Gebeyehu, C.J. Brabec, N.S. Sariciftci, Solid-state organic/inorganic hybrid solar cells based on conjugated polymers and dye-sensitized TiO_2 electrodes, Thin Solid Films 403 (2002) 271–274.
[20] S. Sakaguchi, H. Ueki, T. Kato, T. Kado, R. Shiratuchi, W. Takashima, K. Kaneto, S. Hayase, Quasi-solid dye sensitized solar cells solidified with chemically cross-linked gelators: control of TiO_2/gel electrolytes and counter Pt/gel electrolytes interfaces, J. Photochem. Photobiol. A: Chem. 164 (2004) 117–122.
[21] L. Wang, S.-B. Fang, Y. Lin, Novel polymer electrolytes containing chemically crosslinked gelators for dye-sensitized solar cells, Polym. Adv. Technol. 17 (2006) 512–517.

[22] P. Wang, S.M. Zakeeruddin, I. Exnar, M. Grätzel, High efficiency dye-sensitized nanocrystalline solar cells based on ionic liquid polymer gel electrolyte, Chem. Commun. (2002) 2972–2973.
[23] E. Stathatos, P. Lianos, S.M. Zakeeruddin, P. Liska, M. GrätzelA, Quasi-solid-state dye-sensitized solar cell based on a sol–gel nanocomposite electrolyte containing ionic liquid, Chem. Mater. 15 (2003) 1825.
[24] L. Weiying, K. Junjie, L. Xueping, F. Shibi, L. Yuan, W. Guigiang, X. Xurui, Quasi-solid-state nanocryatallineTiO$_2$ solar cells using gel network polymer electrolytes, Chin. Sci. Bull. 48 (2003) 646–648.
[25] M.-A. De Paoli, A.F. Nogueira, D.A. Machado, C. Longo, All-polymeric electrochromic and photoelectrochemical devices: new advances, Electrochim. Acta 46 (2001) 4243–4249.
[26] Y.J. Kim, J.H. Kim, M.-S. Kang, M.J. Lee, J. Won, J.C. Lee, Y.S. Kang, Supramolecular electrolytes for use in highly efficient dye-sensitized solar cells, Adv. Mater. 16 (2004) 1753–1757.
[27] J.H. Kim, M.-S. Kang, Y.J. Kim, J. Won, N.-G. Park, Y.S. Kang, Dye-sensitized nanocrystalline solar cells based on composite polymer electrolytes containing fumed silica nanoparticles, Chem. Commun. 14 (2004) 1662–1663.
[28] M.-S. Kang, J.H. Kim, Y.J. Kim, J. Won, N.G. Park, Y.S. Kang, Dye-sensitized solar cells based on composite solid polymer electrolytes, Chem. Commun. 7 (2005) 889–891.
[29] M.-S. Kang, J.H. Kim, J. Won, Y.S. Kang, Dye-sensitized solar cells based on crosslinked poly(ethylene glycol) electrolytes, J. Photochem. Photobiol. A: Chem. 183 (2006) 15–21.
[30] M.-S. Kang, J.H. Kim, J. Won, Y.S. Kang, Oligomer approaches for solid-state dye-sensitized solar cells employing polymer, J. Phys. Chem. C 111 (2007) 5222–5228.
[31] E. Chatzivasiloglou, T. Stergiopoulos, A.G. Kontos, N. Alexis, M. Prodromidis, P. Falaras, The influence of the metal cation and the filler on the performance of dye-sensitized solar cells using polymer-gel redox electrolytes, J. Photochem. Photobiol. A: Chem. 192 (2007) 49–55.
[32] Y.H. Liang, C.C. Wang, C.Y. Chen, Comb-like copolymer-based gel polymer electrolytes for lithium ion conductors, J. Power Sources 176 (2008) 340–346.
[33] P.E. Trapa, Y.Y. Won, S.C. Mui, E.A. Olivetti, B.Y. Huang, D.R. Sadoway, A.M. Mayes, S.J. Dallek, Rubbery graft copolymer electrolytes for solid-state, thin-film lithium batteries, J. Electrochem. Soc. 152 (2005) A1–A5.
[34] C. Vandermiers, P. Damman, M. Dosiere, Static and quasielastic light scattering from solutions of poly(ethylene oxide) in methanol, Polymer 39 (1998) 5627–5631.
[35] H. Usui, H. Matsui, N. Tanabe, S. Yanagida, Improved dye-sensitized solar cells using ionic nanocomposite gel electrolytes, J. Photochem. Photobiol. A: Chem. 164 (2004) 97–101.
[36] T. Kato, A. Okazaki, S. Hayase, Latent gel electrolyte precursors for quasi-solid dye sensitized solar cells, Chem. Commun. 3 (2005) 363–365.
[37] T. Kato, T. Kado, S. Tanaka, A. Okazaki, S. Hayase, Quasi-solid dye-sensitized solar cells containing nanoparticles modified with ionic liquid-type molecules, J. Electrochem. Soc. 153 (2006) A626–A630.
[38] L. He, J. Huang, Y. Chen, X. Xu, L. Liu, Inclusion complexation between comb-like PEO grafted polymers and α-cyclodextrin, Macromolecules 38 (2005) 3845–3851.
[39] Y. Takahashi, H. Tadokoro, Structural studies of polyethers, (–(CH$_2$)m–O–)$_n$. X. Crystal structure of poly(ethylene oxide), Macromolecules 6 (1973) 672–675.
[40] S. Sunderrajan, B.D. Freeman, C.K. Hall, I. Pinnau, Propane and propylene sorption in solid polymer electrolytes based on poly(ethylene oxide) and silver salts, J. Membr. Sci. 182 (2001) 1–12.
[41] M.M. Feldstein, A. Roos, C. Chevallier, C. Creton, E.E. Dormidontova, Relation of glass transition temperature to the hydrogen bonding degree and energy in poly(*N*-vinyl pyrrolidone) blends with hydroxyl-containing plasticizers: 3. Analysis of two glass transition temperatures featured for PVP solutions in liquid poly(ethylene glycol), Polymer 44 (2003) 1819–1834.
[42] K. Pielichowski, K. Flejtuch, Differential scanning calorimetry studies on poly(ethylene glycol) with different molecular weights for thermal energy storage materials, Polym. Adv. Technol. 13 (2002) 690–696.
[43] J.H. Park, J.H. Yum, S.Y. Kim, M.S. Kang, Y.G. Lee, S.S. Lee, Y.S. Kang, Cells, J. Photochem. Photobiol. A: Chem. 194 (2008) 148–151.
[44] J.H. Kim, B.R. Min, J. Won, Y.S. Kang, Analysis of the glass transition behavior of polymer–salt complexes: an extended configurational entropy model, J. Phys. Chem. B 107 (2003) 5901–5905.
[45] C. Longo, J. Freitas, M.-A. De Paoli, Performance and stability of TiO$_2$/dye solar cells assembled with flexible electrodes and a polymer electrolyte, J. Photochem. Photobiol. A: Chem. 159 (2003) 33–39.
[46] M.C. Bernard, H. Cachet, P. Falaras, A. Hugot-Le Goff, M. Kalbac, I. Lukes, N.T. Oanh, T. Stergiopoulos, I. Arabatzis, Sensitization of TiO$_2$ by polypyridine dyes, J. Electrochem. Soc. 150 (2003) E155–E164.
[47] G. Schlichthor, S.Y. Huang, J. Sprague, A.J. Frank, Band-edge movement and recombination kinetics in dye-sensitized nanocrystalline TiO$_2$ solar-cells – a study by intensity-modulated photovoltage spectroscopy, J. Phys. Chem. B 101 (1997) 8141–8155.
[48] G. Schlichthorl, N.G. Park, A.J. Frank, Evaluation of the charge-collection efficiency of dye-sensitized nanocrystalline TiO$_2$ solar cells, J. Phys. Chem. B 103 (1999) 782–791.